PERGAMON

Planetary and Space Science 47 (1999) 987–995

Planetary and Space Science

Recent radar observations of asteroid 1566 Icarus

Pravas R. Mahapatra[a], Steven J. Ostro[b,*], Lance A.M. Benner[b], Keith D. Rosema[b], Raymond F. Jurgens[b], Ron Winkler[b], Randy Rose[b], Jon D. Giorgini[b], Donald K. Yeomans[b], Martin A. Slade[b]

[a] *Indian Institute of Science, Bangalore 560012, India*

[b] *Jet Propulsion Laboratory, California Institute of Technology, 4800 Oak Grove Drive, Pasadena, CA 91109-8099, U.S.A.*

Received 1 September 1998; received in revised form 8 January 1999; accepted 15 January 1999

Abstract

We report Doppler-only radar observations of Icarus at Goldstone at a transmitter frequency of 8510 MHz (3.5 cm wavelength) during 8–10 June 1996, the first radar detection of the object since 1968. Optimally filtered and folded spectra achieve a maximum opposite-circular (OC) polarization signal-to-noise ratio of about 10 and help to constrain Icarus' physical properties. We obtain an OC radar cross section of 0.05 km^2 (with a 35% uncertainty), which is less than values estimated by Goldstein (1969) and by Pettengill et al. (1969), and a circular polarization (SC/OC) ratio of 0.5 ± 0.2. We analyze the echo power spectrum with a model incorporating the echo bandwidth B and a spectral shape parameter n, yielding a coupled constraint between B and n. We adopt 25 Hz as the lower bound on B, which gives a lower bound on the maximum pole-on breadth of about 0.6 km and upper bounds on the radar and optical albedos that are consistent with Icarus' tentative QS classification. The observed circular polarization ratio indicates a very rough near-surface at spatial scales of the order of the radar wavelength.

1. Introduction

Radar observations of Apollo asteroid 1566 Icarus during an apparition within 0.043 AU of the Earth in 1968 marked the beginning of asteroid radar astronomy. The encounter caused considerable concern because of unfounded fears of a collision (Nature, 1967; Newsweek, 1968), triggered discussions on ways to counter such collisions (Kleiman, 1968), and led to serious pleas for monitoring asteroids and exploring them by spacecraft (New York Times, 1967, 1968, 1969). A large number of articles were published on the topic during 1967–70 (see website http://pdssbn.astro.umd.edu/SBNast/archive/refs.tab at the University of Maryland, Astronomy Department). Table 1 lists some of the news items and various sorts of articles of the time, indicating the extraordinary level of professional and popular interest generated by the 1968 encounter.

As an asteroid with a relatively long observational history, Icarus' orbit is well known and estimates for many of its physical properties such as its rotation period, diameter, and optical geometric albedo have been reported (Table 2). Its taxonomic classification is uncertain: Tholen (1989) and McFadden et al. (1989; Table 1) do not assign a class, whereas Chapman et al. (1975) prefer an S classification and Hicks et al. (1998) prefer a Q classification (Table 2). From optical observations of polarization and the phase factor of reflectivity, Gehrels et al. (1970) estimated Icarus' geometric albedo to be 0.26, from which they deduced its radius as 0.54 km, assuming a spherical shape. Recently Harris (1998) reanalyzed thermal infrared observations obtained by Veeder et al. (1989) and obtained a diameter of 1.27 km and an optical albedo of 0.33.

With a rotation period of 2.273 h, Icarus is among the fastest known rotators. Rotation periods for only two asteroids have been reported to date that are faster than that of Icarus: 1995 HM with a period of 1.62 h (Steele et al., 1997), and 1998 KY26, which has a rotation period of about 11 min (Ostro et al., 1998; Pravec and Sarounova, 1998; Hicks and Rabinowitz, 1998). Icarus has a perihelion $q = 0.19$ AU that is among the smallest known; the only known asteroids with smaller perihelia are 3200 Phaethon ($q = 0.14$ AU), 1995 CR ($q = 0.12$ AU), and 1998 KN_3 ($q = 0.18$ AU). The small perihelion and the high orbital eccentricity make Icarus a more attractive object than Mercury for testing gravitational theories (Shahid-Salass and Yeomans, 1994). The same orbital parameters have led to speculation that the object

* Corresponding author. Tel.: +1-818-354-3173; fax: +1-818-354-9476; e-mail: ostro@echo.jpl.nasa.gov

0032-0633/99/$ - see front matter
PII: S0032-0633(99)00015-X

Table 1
Selected articles on Icarus' Earth approach in 1968

Title	Publication Details
Interplanetary flight program urged for U.S.	*New York Times*, Aug 15, 1968, p. 17
Monitoring of asteroids urged to warn of impending collisions	*New York Times*, Oct 18, 1967, p. 30
Hippies flee to Colorado as Icarus nears Earth	*New York Times*, June 14, 1968, p.22
Photographs taken of near asteroid	*New York Times*, June 13, 1968, p. 37
23 scientists ask unmanned probe of outer planets	*New York Times*, Aug 4, 1969, p. 1, 11
Prediction of Earth-asteroid collision is scouted	*New York Times*, July 31, 1966, p. 54
The threat of the wandering asteroids	*New York Times*, June 9, 1968, p. 12
Despite cultists, Icarus passes by	*New York Times*, June 15, 1968, p. 39
Astronomers take aim as asteroid nears the Earth	*New York Times*, June 7, 1968, p. 41
Data indicate asteroid Icarus may be a sphere of solid iron	*New York Times*, June 27, 1968, p. 43
Here comes Icarus	*Newsweek* 71, June 17, 1968, p. 74
Whoosh!	*Newsweek* 71, June 24, 1968, p. 74
Icarus in Parliament	*Nature* 216, 1967, p. 529
Icarus passes by	*Nature* 218, 1968, p. 914
Asteroid Icarus flies by the Earth	*Sky and Telescope* 35, 1968, pp. 345, 408
Icarus flies past the Earth	*Sky and Telescope* 36, Aug 1968, pp. 75–77
The nature of Icarus	*Sky and Telescope* 37, Feb 1969, pp. 93–94
Radar echoes from Icarus are received by MIT facility	*IEEE Spectrum* 5, 1968, p. 130
Radar shows Icarus to be tiny, rough	*IEEE Spectrum* 6, 1969, p. 16
Duck, here comes Icarus!	*Science Digest* 62, Oct 1967, p. 33
Can a filmed disaster surpass Earth's peril from space? Icarus	*Science Digest* 85, June 1979, pp. 11–13
Here comes Icarus	*Science Digest* 63, June 1968, pp. 8–14
Icarus, strange swinger	*Science News* 92, Nov 18, 1967, p. 490
Photographs of Icarus	*Spaceflight* 10, 1968, p. 388
Diameter of Icarus believed 900 meters	*Aviation Week & Space Tech*. 90, Jan 6, 1969, p. 77
JPL radar indicates Icarus tiny, very rough	*Rev. Pop. Astron*. 63, Feb. 1969, p. 32
Avoiding an asteroid: when MIT took on Icarus	*Technology Review* 88, July 1985, p. 69
Investigation of the motion of the unusual minor planet Icarus	*Inst. Theo. Astro*. 15, 1984, p. 347
Project Icarus: a book review	*Icarus* 10, 1969, p. 447
Radar observations of Icarus	*Science* 162, 1968, p. 903

may be a spent comet (Gehrels et al., 1970; Weissman et al., 1989).

We observed Icarus in 1996 using an improved Goldstone radar system. This paper presents the results of that study and, while putting them in perspective with the pioneering observations of 1968, touches upon some of the intervening developments.

2. The first radar view

The 1968 apparition of Icarus was observed by Goldstein (1968, 1969) at Goldstone with a continuous-wave (CW) transmission at a frequency of 2388 MHz, and by Pettengill et al. (1969) at 7840 MHz at Haystack. Goldstein (1968) derived a radar cross section (σ_{OC}) of 0.1 km^2 and constrained the radius and rotation period to be 0.3–0.6 km and 1.5–3.3 h. Subsequently the rotation period of Icarus became available through lightcurve studies by Gehrels et al. (1970). Using that result, Goldstein (1969) refined the radius estimate to be $\geqslant$490 m, and constrained the average radar albedo to be $\leqslant$0.13.

Goldstein (1968) reported a splitting of the spectral peak into a bimodal shape as the spectrum evolved during 14–16 June 1968, but Pettengill et al. (1969) did not notice any spectral splitting. Pettengill et al. obtained "a radar cross section of about 0.1 km^2, a radius of 1 km, and an effective reflectivity of about 0.05," with "an uncertainty of about a factor of 2."

3. Intervening developments

Since the first experiments in asteroid radar, numerous developments have occurred in the related disciplines. Upgrades of the Goldstone and Arecibo radars have included transmitter power enhancement, improvements of the antenna and feed structures, and, in the case of the latter, installation of ground interference screening structures. Importantly, both telescopes now have simultaneous dual polarization reception capability, adding a new dimension of information to astronomical observations.

This period has also seen rapid technological development in the areas of data handling, reduction, processing, storage, and display. Automated radar operation and real-time signal and data processing enables more efficient utilization of the limited windows of opportunity

Table 2
A priori information about Icarus[a]

Property	Value	Reference
Semi-major axis (a)	1.078 AU	JPL Solar System Dynamics Database[b]
Eccentricity (e)	0.827	JPL Solar System Dynamics Database[b]
Inclination[c] (i)	22.870°	JPL Solar System Dynamics Database[b]
Taxonomic class	S	Chapman et al. (1975)
	Q	Hicks et al. (1998)
Visual absolute magnitude (H)	15.95	Tedesco (1989)
	16.3 ± 0.3 mag	Harris (1998)[d]
Rotation period (P)	2.25 ± 0.05 h	Veverka and Liller (1969)
	2.268 ± 0.005 h	Miner and Young (1969)
	2.273 ± 0.001 h	Gehrels et al. (1970)
	2.2735 ± 0.0002 h	De Angelis (1995)[f]
Rotation sense	direct	De Angelis (1995)[f]
Maximum light-curve amplitude (Δm)	0.22 mag	Gehrels et al. (1970)
Optical geometric albedo (p_v)	0.33	Harris (1998)[e]
Diameter (D)	1.27 km	Harris (1998)[e]
Principal axis ratio $a/b/c$	1.23/1.0/0.7	De Angelis (1995)[f]
Pole direction	0 ± 3° lat., 49 (or 229) ± 3° long.	Gehrels et al. (1970)
	5 ± 5° lat., 214 ± 5° long.	De Angelis (1995)

[a] Multiple entries for a single parameter or characteristic signify alternative values taken from quoted sources.
[b] http://ssd.jpl.nasa.gov/cgi-bin/et, http://ssd.jpl.nasa.gov/cgi-bin/eph
[c] With reference to J2000 ecliptic
[d] Based on a reanalysis of photometry obtained by Gehrels et al. (1970).
[e] Based on a reanalysis of thermal infrared observations by Veeder et al. (1989).
[f] Based on a reanalysis of photometry obtained by Veverka and Liller (1969), Miner and Young (1969), Gehrels et al. (1970).

for asteroid observation. It is now possible to perform multi-parameter (Range-Doppler-Polarization) observation and processing of asteroid signals, under favorable conditions, to constrain asteroid shapes and surface features (Ostro, 1993; Ostro et al., 1995).

Significant advance has also been made in the knowledge base of asteroid radar signatures and their interpretation, with 37 MBAs (main-belt asteroids) and 49 NEAs observed through the end of 1998. The interpretation of these radar data, by themselves and together with optical and infrared data, have generated a fair degree of understanding regarding the behavior of asteroids of different classes as radar targets and have augmented the fundamental knowledge of these bodies (Ostro et al., 1991a; Ostro, 1994).

Efforts to detect echoes from Icarus at Arecibo in June 1987, when it came within 0.16 AU of the Earth, were unsuccessful. That was the first indication that the actual radar cross section of Icarus may be smaller than 0.1 km^2.

4. A recent radar view

4.1. Data collection and integration

We observed Icarus at Goldstone during 8–12 June 1996. As the echoes were expected to be weak, only CW data were collected during the first three days (Table 3). Each run consisted of transmission of a circularly polarized wave for a period close to the expected

Table 3
Parameters of CW radar data collection

Date	RA (°)	Dec (°)	Runs	Δt(UTC h)	RTT (s)
08 June	338	10	43	11:58–15:52	109
09 June	331	6	27	13:08–14:57	104
10 June	324	2	54	11:52–15:14	101

Data acquisition parameters:
Transmitter frequency (f) = 8510 MHz
Wavelength (λ) = 3.5 cm
Transmitted polarization: RCP
Received polarization: simultaneous OC and SC
Sampling rate: 2 kHz
Basic processing: 1024-point FFT
No. of frequency hops = 4 (Ostro et al., 1992)
Doppler frequency resolution (Δf) = 1.953 Hz

Abbreviations:
Δt: Observation interval
RA: Right ascension
Dec: Declination
RTT: Round Trip Time
RCP: Right Circular Polarization
OC: Opposite Circular Polarization
SC: Same Circular Polarization

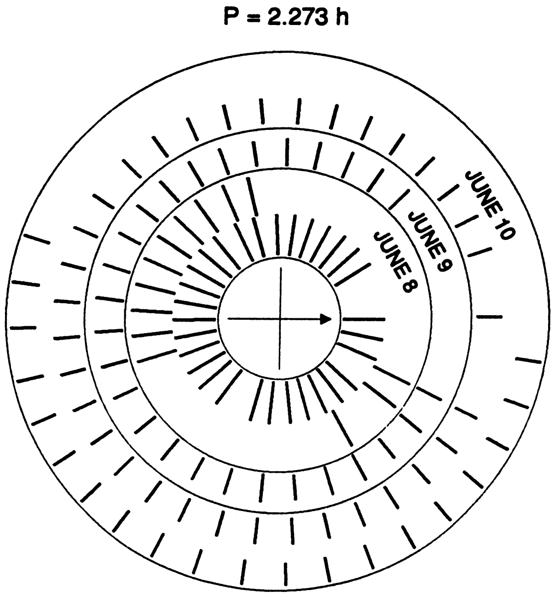

Fig. 1. Relative rotational phase coverage of the CW observations. Each radial line corresponds to the start of the reception for a particular run, and its length is proportional to the standard deviation of the received signal. The first run (11:58 UTC on 8 June 1996) is arbitrarily taken to be at zero phase (along the arrow), and phase increases clockwise.

round-trip light travel time to the target, followed by reception of echoes for a comparable duration. Attempts to obtain range-Doppler echoes on 11 and 12 June using phase-coded transmission were not successful.

The signal-to-noise ratios (SNRs) of the single-run spectra were very weak. We therefore summed the spectra across all the three days. The data covered multiple rotations of Icarus (Fig. 1), so such integration sacrifices rotational resolution.

4.2. Heuristic analysis

We first perform a simple visual analysis of the raw 3-day weighted sum spectra (Fig. 2a). As the SNR in this spectrum is still low (peak SNR ~ 3), we smoothed it with a 10-Hz filter (Fig. 2b), yielding SNR $= \sim 7$. To enhance the SNR even further, we folded the Doppler spectrum about the DC line, (i.e. inverted the spectrum of Fig. 2b about the zero-Doppler axis and added it to the uninverted spectrum). Such an operation on a rotationally averaged spectrum is admissible if the echo's center-of-mass frequency offset is small compared to the spectral resolution, which is the case here. For Icarus, analysis of all available optical and radar astrometry (available on the internet at http://ssd.jpl.nasa.gov/radar.data.html) yields an orbit (http:/ssd.jpl.nasa.gov/cgi-bin/eph) which predicts that the correction to the Goldstone Doppler ephemeris was 0.65 Hz, i.e. $\sim 1/3$ of our raw spectral resolution. The folded spectrum, which has SNR close to 10, is shown in Fig. 2c and indicates an edge-to-edge or zero-crossing bandwidth B of about 45 Hz for the OC spectrum. Since the 10-Hz smoothing would have stretched the bandwidth by about the same amount (i.e. about 10 Hz), the actual value of B is likely to be about 35 Hz. There would also be a small bias in the bandwidth estimate due to the FFT resolution of 1.95 Hz which is neglected.

The lower bound on the size of the asteroid is determined from the equation

$$B(\delta) \leqslant \frac{4\pi D \cos\delta}{\lambda P} \tag{1}$$

where D is the breadth of the plane-of-sky projection of the asteroid's pole-on silhouette, P is its apparent rotation period, δ is the angle between the radar-asteroid line and the equatorial plane of the asteroid, and λ is the radar wavelength. For a lower bound of 35 Hz on B, eqn (1) yields $D \geqslant 0.8$ km.

4.3. Formal analysis

We now make a formal analysis that is more robust against noise effects and explicitly takes into account the radar scattering behavior of Icarus. This is done by least-squares-fitting the unimodal function

$$y(f) = a\left[1 - \left(\frac{f - d_{\text{off}}}{B/2}\right)^2\right]^{\frac{n}{2}} \tag{2}$$

to the raw spectrum, where a is the amplitude of the model function, f is the Doppler frequency, d_{off} is the offset of the center frequency of the target spectrum with respect to the Doppler-prediction ephemeris, and n describes the shape of the echo spectrum. The function (2) corresponds to the spectral shape of the echo signals from a rotating spherical object of uniform surface scattering law modeled as $\cos^n\theta$ where θ is the angle from the incidence direction. In general n depends on the radar backscattering behavior of the asteroid surface with respect to the angle of incidence, the shape of the object, and the reflectivity or 'feature' distribution on the surface. With integration over multiple rotations, n would depend primarily on the average surface backscattering property of a spheroidal asteroid.

Figure 3 shows χ^2 values for the best-fitting model curve over a range of B and n values. A clear minimum exists for any given value of n or B, but the surface has a diagonal trough which defines a coupled constraint for B (and hence D) and n.

As seen from Fig. 2a, the power in the OC and SC spectra varies with a certain degree of independence over the spectral domain, and their ratio μ_c is a function of the particular frequency band chosen. Table 4 shows that μ_c varies between 0.38 and 0.76 over the bandwidths from 15–60 Hz. These high values suggest considerable surface

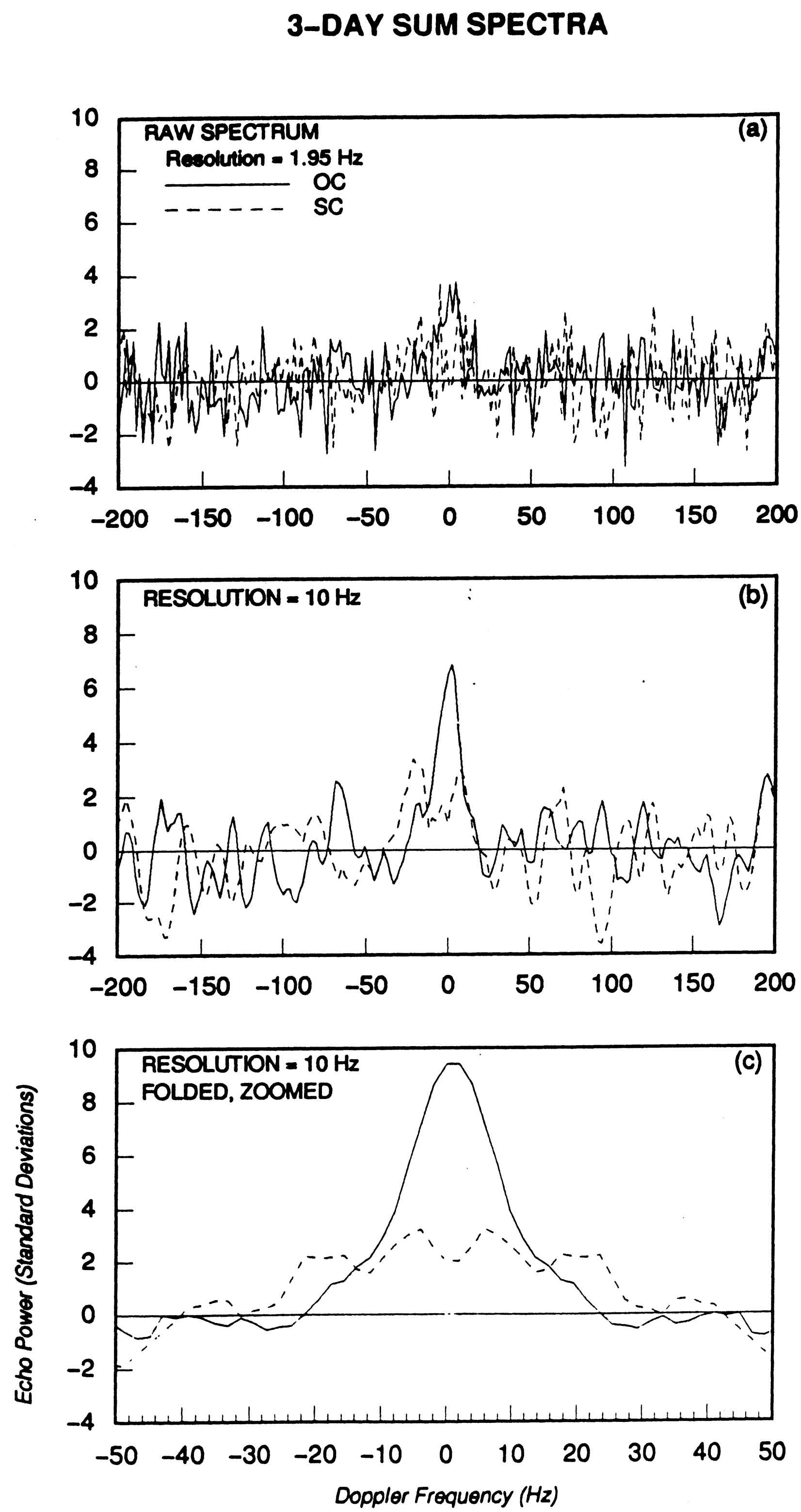

Fig. 2. Weighted sums of all 124 single-run spectra, plotted in terms of noise standard deviation: (a) raw spectra; (b) spectra smoothed to a frequency resolution of 10 Hz; (c) folded and smoothed spectra shown on an expanded scale.

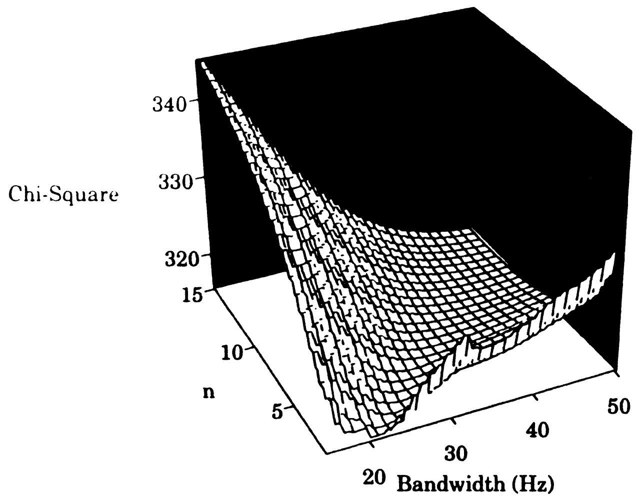

Fig. 3. Chi-square (i.e., the sum of squared residuals) from fitting the spectral model function of eqn (2) to the OC sum spectrum of Fig. 2a, shown as function of bandwidth and spectral shape parameter of the model function. Note the oblique, trough-like minimum.

roughness at spatial scales of the order of λ. One would thus be justified in assuming a fairly diffuse scattering law, possibly with n in the range of 3–5 (this assumption would break down for a sufficiently nonspherical target). The corresponding B from Fig. 3 is between 25 and 35 Hz, with eqn (1) yielding a lower bound for D between 0.57 and 0.77 km for a quasi-spherical shape. The absolute lower bound of 0.57 km is significantly less than the estimates made by both Goldstein (1969) and Pettengill et al. (1969).

If the pole direction obtained by De Angelis (1995, Table 2) is correct, then the sub-radar point on Icarus would have been at latitudes between about -35 and -20 degrees during the observations. If so, then B between 25–35 Hz and D between 0.6–0.8 km should encompass the maximum bandwidth and breadth of Icarus. However, that range of D contradicts the radiometrically-determined diameter of 1.3 km obtained by Harris (1998), suggesting that either the radiometric diameter, the pole direction, or both are incorrect.

4.4. Radar cross section and albedo

Our estimate of Icarus' OC radar cross section, $\sigma_{OC} = 0.050\ km^2 \pm 35\%$, (Table 4), is only about one-half of the 12.5-cm σ_{OC} estimated by Goldstein (1968, 1969) and the 3.8-cm value of $0.1 \pm 0.05\ km^2$ obtained by Pettengill et al. (1969). Since we also observed from Doppler analysis a smaller lower bound for D than earlier estimates, a lower σ_{OC} appears plausible. Within the 1-sigma uncertainties, our radar cross section is consistent with that obtained by Pettengill et al., but we cannot assess the degree to which our value conflicts with the 12.5-cm σ_{OC} because Goldstein did not state the uncertainty in that value. The difference between our radar cross section and Goldstein's nominal value could be due to the difference in the radar wavelengths, the low SNR of both the 1968 and 1996 observations, or to systematic calibration errors.

For each assumed B in Table 4, the radar albedo $\hat{\sigma}_{OC} = \sigma_{OC}/(\pi D^2/4)$ has been calculated using $\sigma_{OC} = 0.050\ km^2$ and D equal to the bound obtained from eqn (1). For the B interval of 25–35 Hz, $\hat{\sigma}_{OC}$ varies from about 0.20 to 0.10, which is in general agreement with $\hat{\sigma}_{OC} \leqslant 0.13$ claimed by Goldstein (1969). Such agreement, however, is the result of our estimates of both σ_{OC} and D being smaller than his by about the same factor. The mean and *rms* dispersion in $\hat{\sigma}_{OC}$ of 13 SQ-class NEAs is 0.14 ± 0.07 (Ostro et al., 1991a, 1996, 1999; Hudson and Ostro,

Table 4
Polarization behavior of Icarus for various bandwidths[a]

Assumed echo bandwidth	Lower bound on diameter, km	OC cross section (σ_{OC}), km^2	SC cross section (σ_{SC}), km^2	Polarization ratio (μ_c) (SC/OC)	OC albedo	Total (OC+SC) albedo
15	0.34	0.038 ± 0.005	0.014 ± 0.003	0.377 ± 0.121	0.412	0.567
20	0.46	0.045 ± 0.006	0.015 ± 0.002	0.335 ± 0.097	0.271	0.304
25	0.57	0.045 ± 0.006	0.021 ± 0.003	0.464 ± 0.130	0.173	0.253
30	0.69	0.052 ± 0.006	0.023 ± 0.003	0.441 ± 0.118	0.139	0.200
35	0.80	0.052 ± 0.006	0.027 ± 0.004	0.518 ± 0.133	0.103	0.157
40	0.92	0.053 ± 0.006	0.030 ± 0.004	0.573 ± 0.145	0.079	0.125
45	1.03	0.054 ± 0.006	0.033 ± 0.004	0.624 ± 0.155	0.064	0.104
50	1.15	0.051 ± 0.006	0.036 ± 0.005	0.714 ± 0.172	0.049	0.084
55	1.26	0.050 ± 0.006	0.038 ± 0.005	0.756 ± 0.182	0.040	0.070
60	1.38	0.050 ± 0.006	0.034 ± 0.004	0.681 ± 0.161	0.033	0.056

[a] Based on the raw 3-day-sum OC and SC spectra with 1.95 Hz resolution. The uncertainties quoted herein reflect the variances due to the statistical nature of the signal, and do not reflect the radar calibration errors, which raise the fraction uncertainty to ~35%.

1994), so our $\hat{\sigma}_{OC}$ estimate for Icarus is consistent with its classification as an SQ-type object.

4.5. Correlation with visual albedo

Figure 4 shows a plot of $\hat{\sigma}_{OC}$ as a function of D and depicts the variation of the visual geometric albedo p_v for $H = 16.3$ (Table 2). p_v is obtained from the relation (Zellner, 1979)

$$\log p_v = 6.244 - 2\log D - 0.4H. \quad (3)$$

Also marked on the $\hat{\sigma}_{OC}$-D curves in Fig. 4 are the points whose ordinates correspond to the average radar albedo of NEAs and MBAs by taxonomic class. The lower bound of 0.57 km on the pole-on breadth of Icarus corresponds to an upper bound on $\hat{\sigma}_{OC}$ of 0.20 that is in the middle of the known asteroid radar albedo distribution. However, if the radiometric diameter of 1.27 km obtained by Harris (1998) is correct, then the radar albedo of Icarus is about 0.04, which is the lowest radar albedo estimated for any S-class main-belt or near-Earth asteroid to date. That estimate is also comparable to the radar albedo of comet IRAS-Araki-Alcock (0.04; Harmon et al., 1989), although visible spectroscopy does not suggest that Icarus is a comet.

4.6. Polarization ratio

In the B interval of 25–35 Hz, μ_c is observed from Table 4 to be between 0.44 and 0.52. Even after accounting for the estimation uncertainty of 12–13%, these values are high for NEAs, but are not unique. Ostro et al. (1991b) provide μ_c values for 29 NEAs (at $\lambda = 3.5$ and 13 cm) which have a mean of 0.3 and 1-sigma dispersion of 0.22, with five objects yielding $\mu_c \geqslant 0.42$. Specifically, NEAs that have larger circular polarization ratios at $\lambda = 3.5$ cm are 1981 Midas ($\mu_c \sim 0.65$) and 3908 (1980 PA) ($\mu_c \sim 0.72$). Further, the asteroids 2101 Adonis, 3103 Eger, and 1992 QN have recently been found to have near-unity circular polarization ratios (Benner et al., 1997). If we adopt $\mu_c = 0.5 \pm 0.2$ as a nominal value for Icarus, then the 1-sigma lower bound on the circular

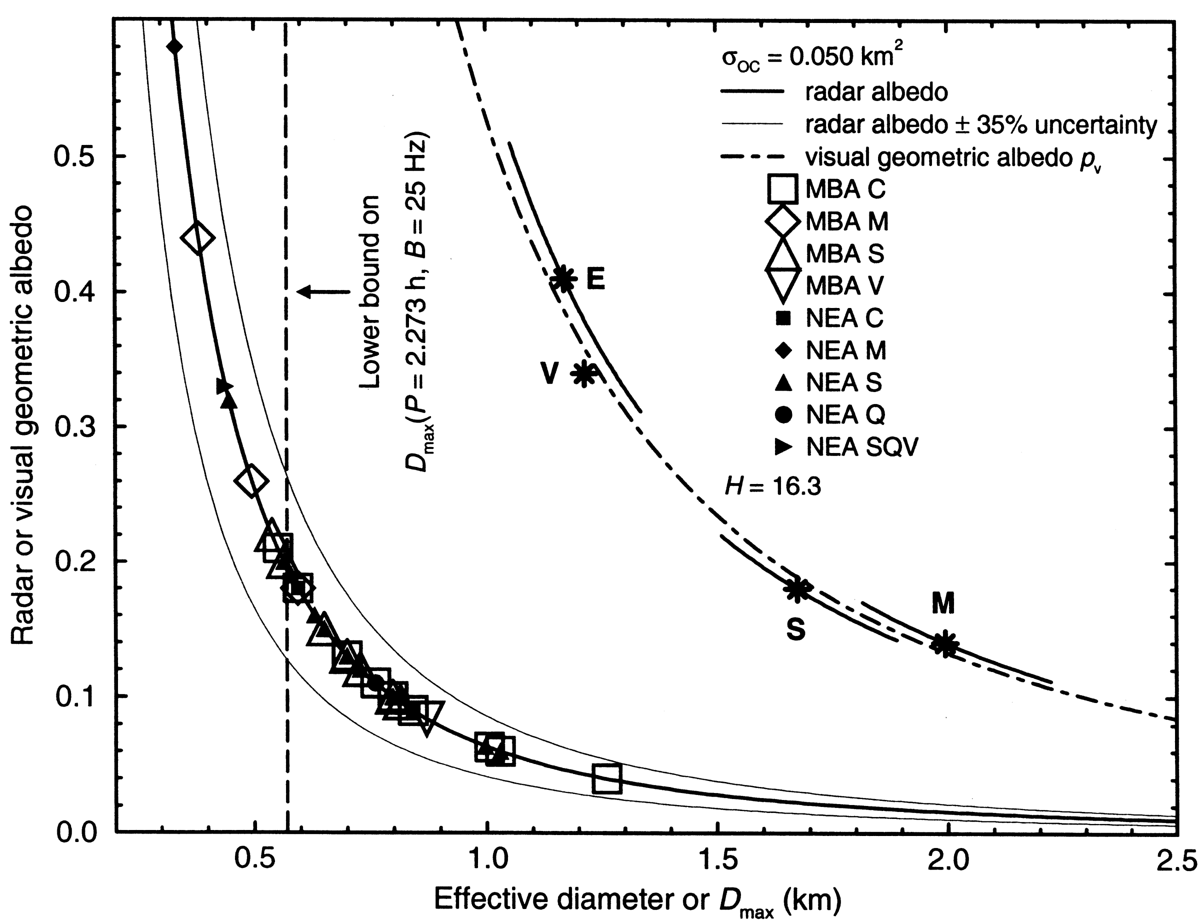

Fig. 4. Radar albedo (dark solid curve) of Icarus as a function of its effective diameter, calculated with our estimated radar cross-section $\sigma_{OC} = 0.050$ km^2. This curve is bounded by thin solid lines representing $\pm 35\%$ uncertainty. The radar albedos of near-Earth and main-belt asteroids are superimposed on the radar albedo curve. The visual geometric albedo is also plotted (dash-dot line) for $H = 16.3$ (Harris, 1998). The asterisks and their accompanying thick solid curve segments represent, respectively, the mean and rms dispersion of the visual geometric albedos for principal taxonomic classes (Tedesco, 1989).

polarization ratio of Icarus exceeds about 70% of the values reported for S-class asteroids so far (28 objects), suggesting that Icarus has a near-surface that is among the roughest at centimeter-to-decimeter spatial scales observed among all S-class asteroids. This high degree of small-scale roughness may or may not arise from regolith structure. Although small and rapidly rotating asteroids are less likely to have loose surface regolith, McFadden et al. (1989) suggest that several NEAs do support regoliths (perhaps dusty), and that: "the controlling factors of regolith properties and processes are not simply due to scaling with size and gravity." In the case of Icarus, based on its size and rotation period, the existence of surface regolith is plausible if Icarus' density is greater than 1 g cm^{-3}, which is a reasonable assumption given that the smallest asteroid density presently known is 1.3 g cm^{-3} for 253 Mathilde (Yeomans et al., 1997).

5. Conclusion

The SNR of the 1996 observations was not substantially better than those obtained during the first observations in 1968. Icarus was farther from the Earth in 1996 than in 1968 by a factor of 2.4, which, by the inverse-fourth-power dependence of the SNR on range, would yield an echo power over 30 times weaker if all other parameters remained invariant. It is due to the advances in the radar capabilities during the intervening decades that the 1996 observations' SNR was possible.

The next radar opportunity to observe Icarus will be in June 2015 when the asteroid will pass within 0.054 AU of Earth. Estimated SNRs per date in 2015 at Arecibo should approach $\sim$2000, adequate for a 3-D shape reconstruction with decameter resolution.

Acknowledgements

We thank Alan Harris (JPL) and John Harmon (NAIC) for helpful reviews. Pravas R. Mahapatra and Lance A.M. Benner were supported as Research Associates of the National Research Council at JPL. Part of this research was conducted at the Jet Propulsion Laboratory, California Institute of Technology, under contract with the National Aeronautics and Space Administration (NASA).

References

Benner, L.A.M., Ostro, S.J., Giorgini, J.D., Jurgens, R.F., Mitchell, D.L., Rose, R., Rosema, K.D., Slade, M.A., Winkler, R., Yeomans, D.K., Campbell, D.B., Chandler, J.F., Shapiro, I.I., 1997. Radar detection of near-Earth asteroids 2062 Aten, 2101 Adonis, 3103 Eger, 4544 Xanthus, and 1992 QN. Icarus 130, 296–312.

Chapman, C.R., Morrison, D., Zellner, B., 1975. Surface properties of asteroids: A synthesis of polarimetry, radiometry, and spectrophotometry. Icarus 25, 104–130.

Chapman, C.R., Harris, A.W., Binzel, R., 1994. Physical properties of near-Earth asteroids: Implications for the hazard issue. In: Gehrels, T., (Ed.), Hazards due to Comets and Asteroids, University of Arizona Press, Tucson, pp. 537–549.

De Angelis, G., 1995. Asteroid spin, pole and shape determinations. Planet. Space Sci. 43, 649–682.

Gehrels, T., Roemer, E., Taylor, R.C., Zellner, B.H., 1970. Minor planets and related objects. IV. Asteroid (1566) Icarus. Astron. J. 75, 186–195.

Goldstein, R.M., 1968. Radar observations of Icarus. Science 162, 903–904.

Goldstein, R.M., 1969. Radar observations of Icarus. Icarus 10, 430–431.

Harmon, J.K., Campbell, D.B., Hine, A.A., Shapiro, I.I., Marsden, B.G., 1989. Radar observations of comet IRAS-Araki-Alcock 1983d. Astrophys. J. 338, 1071–1093.

Harris, A.W., 1998. A thermal model for near-Earth asteroids. Icarus 131, 291–301.

Hicks, M.D., Fink, U., Grundy, W.M., 1998. The unusual spectra of 15 near-Earth asteroids and extinct comet candidates. Icarus 133, 69–78.

Hicks, M., Rabinowitz, D., 1998. IAU Circ. 6935.

Hudson, R.S., Ostro, S.J., 1994. Shape of asteroid 4769 Castalia (1989 PB) from inversion of radar images. Science 263, 940–943.

Kleiman, L.A., 1968. (Ed.) Project Icarus. M.I.T. Report No. 13. The M.I.T. Press, Cambridge, Massachusetts, pp. 121.

Lagerkvist, C.-I., Harris, A.W., Zappala, V., 1989. Asteroid lightcurve parameters. In: Binzel, R.P., Gehrels, T., Matthews, M.S., (Eds.), Asteroids II, University of Arizona Press, Tucson, pp. 1162–1179.

McFadden, L.-A., Tholen, D.J., Veeder, G.J., 1989. Physical properties of Aten, Apollo and Amor asteroids. In: Binzel, R.P., Gehrels, T., Matthews, M.S., (Eds.), Asteroids II, University of Arizona Press, Tucson, pp. 442–467.

Miner, E., Young, J., 1969. Photometric determination of the rotation period of 1566 Icarus. Icarus 10, 436–440.

Nature, 1967. Icarus in Parliament. Nature 216, 529 (News Item).

Newsweek, 1968. Here comes Icarus. 71, June 17, p. 74.

New York Times, 1967. Monitoring of asteroids urged to warn of impending collisions. Oct. 18, p. 30.

New York Times, 1968. Interplanetary flight program urged for U.S. Aug. 15, p. 17.

New York Times, 1969. 23 scientists ask unmanned probe of outer planets. Aug. 4, pp. 1, 11.

Ostro, S.J., 1993. Planetary radar astronomy. Rev. Mod. Phys. 65, 1235–1279.

Ostro, S.J., Benner, L., Giorgini, J., Rosema, K., Yeomans, D., 1998. IAU Circ. 6935.

Ostro, S.J., Campbell, D.B., Chandler, J.F., Hine, A.A., Hudson, R.S., Rosema, K.D., Shapiro, I.I., 1991a. Asteroid 1986 DA: Radar evidence for a metallic composition. Science 252, 1399–1404.

Ostro, S.J., Campbell, D.B., Chandler, J.F., Shapiro, I.I., Hine, A.A., Velez, R., Jurgens, R.F., Rosema, K.D., Winkler, R., Yeomans, D.K., 1991b. Asteroid radar astrometry. Astron. J. 102, 1490–1502.

Ostro, S.J., Campbell, D.B., Simpson, R.A., Hudson, R.S., Chandler, J.F., Rosema, K.D., Shapiro, I.I., Standish, E.M., Winkler, R., Yeomans, D.K., Velez, R., Goldstein, R.M., 1992. Europa, Ganymede, and Callisto: New radar results from Arecibo and Goldstone. J. Geophys. Res. 97 No. E11, 18,227–18,244.

Ostro, S.J., Hudson, R.S., Jurgens, R.F., Rosema, K.D., Campbell, D.B., Yeomans, D.K., Chandler, J.F., Giorgini, J.D., Winkler, R., Rose, R., Howard, S.D., Slade, M.A., Perillat, P., Shapiro, I.I., 1995. Radar images of asteroid 4179 Toutatis. Science 270, 80–83.

Ostro, S.J., Jurgens, R.F., Rosema, K.D., Hudson, R.S., Giorgini, J.D., Winkler, R., Yeomans, D.K., Choate, D., Rose, R., Slade, M.A.,

Howard, S.D., Scheeres, D.J., Mitchell, D.L., 1996. Radar observations of asteroid 1620 Geographos. Icarus 121, 46–66.
Ostro, S.J., Hudson, R.S., Rosema, K.D., Giorgini, J.D., Jurgens, R.F., Yeomans, D.K., Chodas, P.W., Winkler, R., Rose, R., Choate, D., Cormier, R.A., Kelley, D., Littlefair, R., Benner, L.A.M., Thomas, M.L., Slade, M.A., 1999. Asteroid 4179 Toutatis: 1996 radar observations. Icarus 137, 122–139.
Pettengill, G.H., Shapiro, I.I., Ash, M.E., Ingalls, R.P., Rainville, L.P., Smith, W.B., Stone, M.L., 1969. Radar observations of Icarus. Icarus 10, 432–435.
Pravec, P., Sarounova, L., 1998. IAU Circ. 6941.
Shahid-Salass, B., Yeomans, D.K., 1994. Relativistic effects on the motion of asteroids and comets. Astronomical J. 107, 1885–1889.
Steele, D.I., McNaught, R.H., Garradd, G.J., Asher, D.J., Taylor, A.D., 1997. Near-Earth asteroid 1995 HM: A highly-elongated monolith rotating under tension? Planet. Space Sci. 45, 1091–1098.
Tedesco, E.F., 1989. Asteroid magnitudes, UBV colors, and IRAS albedos and diameters. In: Binzel, R.P., Gehrels, T., Matthews, M.S., (Eds.), Asteroids II, University of Arizona Press, Tucson, pp. 1090–1138.
Tholen, D.J., 1989. Asteroid taxonomic classifications. In: Binzel, R.P., Gehrels, T., Matthews, M.S., (Eds.), Asteroids II, University of Arizona Press, Tucson, pp. 1139–1150.
Veeder, G.J., Hanner, M.S., Matson, D.L., Tedesco, E.F., Lebofsky, L.A., Tokunaga, A.T., 1989. Radiometry of near-Earth asteroids. Astron. J. 97, 1211–1219.
Veverka, J., Liller, W., 1969. Observations of Icarus: 1968. Icarus 10, 441–444.
Weissman, P.R., A'Hearn, M.F., McFadden, L.A., Rickman, H., 1989. Evolution of comets into asteroids. In: Binzel, R.P., Gehrels, T., Matthews, M.S., (Eds.), Asteroids II, University of Arizona Press, Tucson, pp. 880–920.
Yeomans, D.K., Barriot, J.-P., Dunham, D.W., Farquhar, R.W., Giorgini, J.D., Helfrich, C.E., Konopliv, A.S., McAdams, J.V., Miller, J.K., Owen Jr., W.M., Scheeres, D.J., Synott, S.P., Williams, B.G., 1997. Estimating the mass of asteroid 253 Mathilde from tracking data during the NEAR flyby. Science 278, 2106–2109.
Zellner, B., 1979. Asteroid taxonomy and the distribution of the compositional types. In: Gehrels, T., (Ed.), Asteroids, University of Arizona Press, Tucson, pp. 783–806.